Geochemistry Geophysics Geosystems G3
AN ELECTRONIC JOURNAL OF THE EARTH SCIENCES
Published by AGU and the Geochemical Society

Article
Volume 9, Number 1
12 January 2008
Q01004, doi:10.1029/2007GC001683
ISSN: 1525-2027

Abrupt changes of temperature and water chemistry in the late Pleistocene and early Holocene Black Sea

André Bahr
MARUM-Zentrum für Marine Umweltwissenschaften der Universität Bremen, Postfach 330440, D-28334 Bremen, Germany (bahr@uni-bremen.de)

Frank Lamy
AWI Bremerhaven, Am Handelshafen 12, D-27570 Bremerhaven, Germany

Helge W. Arz
Section 3.3, GeoForschungsZentrum-Potsdam, Telegrafenberg, D-14473 Potsdam, Germany

Candace Major
Geology and Geophysics, Woods Hole Oceanographic Institution, Woods Hole, Massachusetts 02543, USA

Olga Kwiecien
Section 3.3, GeoForschungsZentrum-Potsdam, Telegrafenberg, D-14473 Potsdam, Germany

Gerold Wefer
MARUM-Zentrum für Marine Umweltwissenschaften der Universität Bremen, Postfach 330440, D-28334 Bremen, Germany

[1] New Mg/Ca, Sr/Ca, and published stable oxygen isotope and $^{87}Sr/^{86}Sr$ data obtained on ostracods from gravity cores located on the northwestern Black Sea slope were used to infer changes in the Black Sea hydrology and water chemistry for the period between 30 to 8 ka B.P. (calibrated radiocarbon years). The period prior to 16.5 ka B.P. was characterized by stable conditions in all records until a distinct drop in $\delta^{18}O$ values combined with a sharp increase in $^{87}Sr/^{86}Sr$ occurred between 16.5 and 14.8 ka B.P. This event is attributed to an increased runoff from the northern drainage area of the Black Sea between Heinrich Event 1 and the onset of the Bølling warm period. While the Mg/Ca and Sr/Ca records remained rather unaffected by this inflow; they show an abrupt rise with the onset of the Bølling/Allerød warm period. This rise was caused by calcite precipitation in the surface water, which led to a sudden increase of the Sr/Ca and Mg/Ca ratios of the Black Sea water. The stable oxygen isotopes also start to increase around 15 ka B.P., although in a more gradual manner, due to isotopically enriched meteoric precipitation. While Sr/Ca remains constant during the following interval of the Younger Dryas cold period, a decrease in the Mg/Ca ratio implies that the intermediate water masses of the Black Sea temporarily cooled by 1–2°C during the Younger Dryas. The $^{87}Sr/^{86}Sr$ values drop after the cessation of the water inflow at 15 ka B.P. to a lower level until the Younger Dryas, where they reach values similar to those observed during the Last Glacial Maximum. This might point to a potential outflow to the Mediterranean Sea via the Sea of Marmara during this period. The inflow of Mediterranean water started around 9.3 ka B.P., which is clearly detectable in the abruptly increasing Mg/Ca, Sr/Ca, and $^{87}Sr/^{86}Sr$ values. The accompanying increase in the $\delta^{18}O$ record is less pronounced and would fit to an inflow lasting ~100 a.

Components: 10,804 words, 7 figures, 2 tables.

Keywords: Black Sea; ostracods; trace elements.

Index Terms: 0473 Biogeosciences: Paleoclimatology and paleoceanography (3344, 4900); 3344 Atmospheric Processes: Paleoclimatology (0473, 4900); 4243 Oceanography: General: Marginal and semi-enclosed seas; 4835 Oceanography: Biological and Chemical: Marine inorganic chemistry (1050); 1050 Geochemistry: Marine geochemistry (4835, 4845, 4850).

Received 9 May 2007; **Revised** 1 October 2007; **Accepted** 23 October 2007; **Published** 12 January 2008.

Bahr, A., F. Lamy, H. W. Arz, C. Major, O. Kwiecien, and G. Wefer (2008), Abrupt changes of temperature and water chemistry in the late Pleistocene and early Holocene Black Sea, *Geochem. Geophys. Geosyst.*, *9*, Q01004, doi:10.1029/2007GC001683.

1. Introduction

[2] Today the Black Sea is the largest semi-enclosed basin of the world (V = 537,000 km^3) that is only connected with the global ocean through the ~36 m deep Bosphorus strait. This particular situation led to a complete disconnection with the open ocean during the last glacial period, when the global sea level was lower than the Bosphorus sill. As a consequence the Black Sea turned into a fresh or slightly brackish lake [*Mudie et al.*, 2002a] in which its hydrology and lake level were very sensitive to environmental changes.

[3] One of the major environmental variables is the freshwater budget of the Black Sea, which contributed to significant sea level oscillations since the glacial period [e.g., *Ryan et al.*, 1997, 2003; *Aksu et al.*, 2002]. Previous publications proposed the inflow of large amounts of meltwater from Scandinavian and/or Siberian ice sheets into the Black Sea after the LGM [*Ryan et al.*, 2003; *Mangerud et al.*, 2004; *Bahr et al.*, 2006; *Major et al.*, 2006] that were inferred to result in an overflow of the Black Sea into the Sea of Marmara [*Kvasov*, 1979] and to a temporary freshening of the Sea of Marmara [*Mudie et al.*, 2003]. A further direct response to climatic changes is the precipitation of calcite during the Bølling/Allerød (B/A) and early Holocene [*Major et al.*, 2002; *Bahr et al.*, 2005] as a result of CO_2-assimilation through enhanced phytoplankton activity during favorable climatic conditions.

[4] Due to the large volume of the Black Sea, variations in the stable oxygen isotopic composition of the water body are slow and, during its lacustrine stage, mainly governed by changes in the isotopic composition of precipitation and runoff [*Bahr et al.*, 2006]. Stable oxygen isotope records based on ostracod and bivalve shells from different water depths [*Bahr et al.*, 2006; *Major et al.*, 2006] and bulk δ^{18}O data [*Major et al.*, 2002] suggest that the effect of temperature changes is rather restricted to the uppermost water column. These data also imply that the water column experienced periods with vertical stratification, but without developing anoxic conditions in the deeper basin.

[5] However, the effects, if any, these environmental changes had on the water chemistry and temperature evolution of the Black Sea are not well known until now. Here we present newly obtained Mg/Ca and Sr/Ca measurements on ostracod shells from the western Black Sea that, in combination with previously published δ^{18}O and ^{87}Sr/^{86}Sr data (on biogenic calcite), reveal abrupt changes in the water chemistry of the Black Sea in terms of its elemental composition in response to climatic and hydraulic changes between the Last Glacial Maximum and the early Holocene. A particular focus lies in this case on the deglacial period and the reconnection of the Black Sea with the global ocean at circa 9.3 ka cal B.P. The combination of Sr/Ca and Mg/Ca ratios allows furthermore for semi-quantitative estimates on temperature variability in the deep Black Sea, which has not been assessed so far. On the basis of a newly defined age model [*Kwiecien et al.*, 2008] we also re-evaluate the previously discussed influences of potential meltwater incursions into the Black Sea.

2. Environmental Setting

[6] At present the water balance of the Black Sea is positive: freshwater sources (300 km^3 a^{-1} precipitation and 350 km^3 a^{-1} runoff, of which 190 km^3 a^{-1} is contributed by the Danube [*Panin and Jipa*, 2002]) exceed the losses by evaporation (350 km^3 a^{-1}) [*Swart*, 1991]. The remaining components of the freshwater budget are compensated

Table 1. Location and Length of the Investigated Gravity Cores

Core Name	Latitude N	Longitude E	Water Depth, m	Core Length, cm
GeoB 7604-2	42°56.2′	30°01.9′	1977	592
GeoB 7607-2	43°09.7′	29°57.7′	1562	636
GeoB 7608-1	43°29.2′	30°11.8′	1202	685
GeoB 7609-1	43°32.8′	30°09.2′	941	655
GeoB 7610-1	43°38.9′	30°04.1′	465	880
MD04-2760	41°31.7′	30°53.1′	1226	4204
MD04-2788	41°31.7′	30°53.0′	1224	600

by the net flux of warm, salty water through the Bosphorus from the Sea of Marmara [*Öszoy and Ünlüata*, 1997]. The high amount of freshwater input to the Black Sea is also responsible for its particular hydrographic situation. A stable pycnocline between 100 and 200 m water depth separates less saline near-surface water (18‰ salinity) from the more saline (22.5‰) deep water of Mediterranean origin. Due to this stable stratification, anoxic conditions prevail below a depth of ~150 m. The stable isotope composition of Black Sea waters reflects the present hydrology with values around −2.8‰ in the upper 50 m and −1.8‰ in depths >500 m [*Öszoy et al.*, 2002]. In areas with significant freshwater influence, like in our research area, $\delta^{18}O$ values are depleted (−10.5‰ near the Danube river mouth and −3‰ on the NW Black Sea shelf close to the coring sites [*Öszoy et al.*, 2002]).

[7] The present-day values of Black Sea water for Sr/Ca (7.68 mmol/mol in 2000 m water depth [*Aloisi et al.*, 2004]) and Mg/Ca (4.55 mol/mol for the surface waters, 4.77 mol/mol in 2000 m water depth [*Manheim and Chan*, 1974]) approach typical marine ratios (Sr/Ca: 8.74 mmol/mol; Mg/Ca: 5.16 mol/mol [*Chester*, 1990]), but the freshwater influence on the upper water column is still expressed in the slightly reduced Mg/Ca ratio of surface water relative to the deep water. In areas of dominant freshwater input, like the Danube Delta, the Mg/Ca ratio can be as low as 0.612 mol/mol [*Manheim and Chan*, 1974]. The average $^{87}Sr/^{86}Sr$ ratio of mollusk shells from core top samples from the Black Sea (0.709133 ± 0.000015) [*Major et al.*, 2006] is close to that measured on modern shells from the fully marine Aegean Sea (0.709157 ± 0.00001) but still indicates a slight influence of Sr brought in by rivers [*Major et al.*, 2006].

3. Material and Methods

[8] This study is based on five gravity cores from the NW Black Sea, retrieved during R/V *Meteor* cruise M51-4 [*Jørgensen*, 2003]. They are located on a depth transect ranging from the upper (465 m water depth) to the lower continental slope (1977 m) (Table 1 and Figure 1). The cores from the slope contain the classical sequence of the marine units I (finely laminated coccolith ooze) and II (sapropelic sediments) in the top ~45 cm, and the lacustrine unit III (homogeneous to (mostly) mm-scale laminated muddy clay) in the lower part of the cores [*Bahr et al.*, 2005].

[9] All GeoB cores listed in Table 1 were analyzed in 1 cm resolution with a CORTEX X-ray fluorescence (XRF) scanner measuring the K, Ca, Ti, Mn, Fe, Cu and Sr contents in counts per second, while core MD04-2760 has been scanned with an AVAA-TECH-Scanner giving XRF-intensities in total counts; both scanners are located at the University of Bremen [*Jansen et al.*, 1998; *Röhl and Abrams*, 2000, *Richter et al.*, 2006]. Stable isotope analyses ($\delta^{18}O$ and $\delta^{13}C$) were performed on 5–8 shells of juvenile ostracods belonging to the genus *Candona* spp. (for further details, see *Bahr et al.* [2006]) at the University of Bremen.

[10] Total carbon (TC) was measured on freeze-dried samples using a LECO SC-444 instrument. Total inorganic carbon (TIC) was determined using a CM 5012 CO_2 coulometer with a CM5140 acidification device. TOC contents were calculated from the difference between TC and TIC. These measurements were done at the ICBM, Oldenburg, Germany.

[11] For Mg/Ca and Sr/Ca analysis 3 to 10 ostracod valves of the species *Candona schweyeri* (adult) were picked from the 150 μm fraction. Each valve was cleaned individually in a faunal slide under the microscope with a fine brush and a few drops of deionized water. The cleaning procedure was repeated three times, after each cleaning the samples were immediately dried to avoid corrosion of the shell by deionized water. Valves were subsequently dissolved in 2% HNO_3 and measured with a

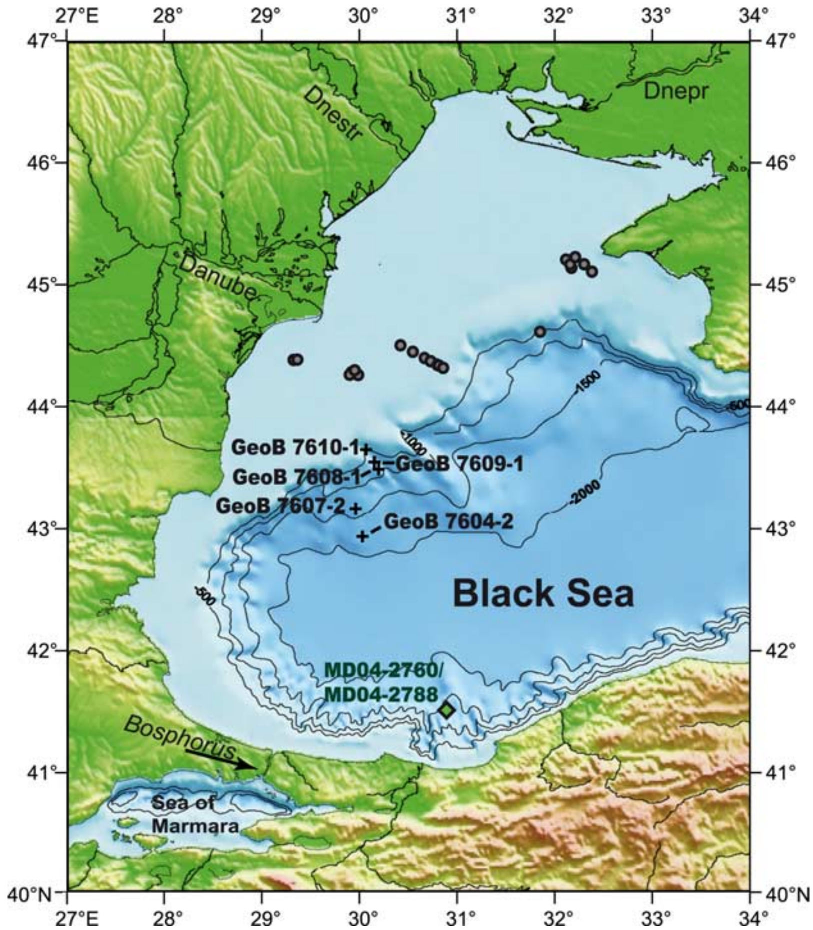

Figure 1. Location of gravity cores retrieved during R/V *Meteor* cruise M51-4 in 2001 (crosses) and on board R/V *Marion Dufresne* during the ASSEMBLAGE I cruise in 2004 (diamonds) and those of *Major et al.* [2006] (circles).

Finnigan Element2 ICP-MS at the Woods Hole Oceanographic Institution (WHOI). The average analytical precision from replicates was 2.9% for Mg/Ca and 1.7% for Sr/Ca.

[12] All data are available under the name of the corresponding author through the PANGAEA server (http://www.pangaea.de/PangaVista).

4. Age Model

[13] An age model was developed for core GeoB 7608-1 based on 6 AMS ^{14}C dates calibrated to calendar years B.P. (1950) with the program Calib Rev 5.0.1 [*Stuiver and Reimer*, 1993] using the INTCAL04 calibration curve [*Reimer et al.*, 2004] (Table 2). In the previously used stratigraphy for GeoB 7608-1 [*Bahr et al.*, 2005, 2006] a constant 1000 a reservoir age correction throughout the record was assumed, however, new findings made modifications of this earlier stratigraphy necessary.

[14] The first modification is based on the discovery of the Y-2 tephra from the Cape Riva eruption of the Santorini volcano 21,780 ± 510 a cal B.P. ago [*Eriksen et al.*, 1990; *Pilcher and Friedrich*, 1976] in core MD04-2760 from the southwestern Black Sea (Figure 1). Radiocarbon dated samples of ostracod shells bracketing the Y-2 tephra in core MD04-2760 imply that the reservoir age of the glacial Black Sea was approximately 1450 a [*Kwiecien et al.*, 2008]. On the basis of a comparison of MD04-2760 with the Greenland ice core records a drop of the reservoir age to 900–1000 a seems to occur before the onset of the Bølling [*Kwiecien et al.*, 2008]. The sedimentary sequences of cores GeoB 7608-1 and MD04-2760 can be correlated very well using the XRF-scanning data [*Kwiecien et al.*, 2008] (Ca abundances are shown in Figure 2; the correlation was performed visually also using K and Ti/Ca curves with the program ICC by Norbert Nowaczyk, GFZ-Potsdam). On the basis of this correlation it was argued that the radiocarbon dates from 436 cm (18,257 ± 305 a

Table 2. Age Control Points for GeoB 7608-1

Lab. ID	Core Depth, cm	^{14}C Age, a B.P.	Calendar Age, a B.P.	Age, Tuned to MD04-2760, a B.P.	Material
	31		7995		Unit II/III boundary [*Lamy et al.*, 2006]
KIA 21464	34	7735 ± 50	8116 ± 100[a]		Ostracods
KIA 21463	88	11,460 ± 70	12,394 ± 280[b]		Gastropod
KIA 21461	158	13,350 ± 80	14,240 ± 345[b]		Gastropod
KIA 21460[c,d]	243	17,080 + 150/−140	18,899 ± 230[e]	14,683	Ostracods and bivalves
KIA 21866[d]	436	16,360 ± 70	18,257 ± 305[e]	15,795	Ostracods and bivalves
KIA 21459[d]	596	20,140 + 180/−170	22,197 ± 425[e]	22,567	Gastropod
KIA 21457[d]	652	24,970 + 310/−300	28,488 ± 485[e]	24,928	Mixed mollusk shells

[a] Calculated with 415 a reservoir correction.
[b] Calculated with 1000 a reservoir correction.
[c] Sample was discarded because of its high amount of broken and probably reworked shells [*Bahr et al.*, 2006].
[d] Dates were not used because of the adoption of the stratigraphy from MD04-2760 [*Kwiecien et al.*, 2008] (see also Figure 2).
[e] Calculated with 1450 a reservoir correction [*Kwiecien et al.*, 2008].

cal B.P.) and 652 cm (28,488 ± 485 a cal B.P.) were much too old, perhaps by contamination with reworked shells [*Kwiecien et al.*, 2008], while the dating from 596 cm (22,197 ± 425 a cal B.P.) lies within the error estimates, possibly a result of the better dating material (a whole gastropod shell). Following this assumption and considering the higher number of radiocarbon dates we decided to tune the pre-Bølling part (i.e., the part older than 14,240 a cal B.P.; see also Table 2) of GeoB 7608-1 to MD04-2760, also discarding the dating from 596 cm for reasons of consistency. This has important consequences for the chronological position of the reddish clay layers interpreted to be deposited during the inflow of meltwater from the Fennoscandian Ice Sheet (FIS). On the basis of our new stratigraphy, the deposition of the clay layers started significantly later at 16.5 and lasted until 14.8 ka cal B.P. (compared to 18 and 15.5 ka cal B.P. [*Bahr et al.*, 2005]; see also Figure 4i). The second modification affects the age of the Unit II/III boundary, that was previously positioned at circa 7.5 ka B.P. [*Jones and Gagnon*, 1994], using organic matter and inorganic carbon as dating material. However, new datings on a core from the southwestern Black Sea [*Lamy et al.*, 2006], performed on planktonic larval shells of the bivalve *Mytilus galloprovinciales*, suggest that this boundary is ~8.0 ka old. This is significantly older than the calibrated age of 7610 ± 40 a B.P. (calculated using the 1000 a reservoir age correction) from core GeoB 7608-1 (7735 ± 50 ^{14}C a B.P.) taken just below the Unit II/Unit III boundary at 34 cm. This discrepancy might be resolved if a lower reservoir age correction is applied to this date: an extreme estimate is 415 a, the reservoir age calculated for the marine Black Sea [*Siani et al.*, 2001], which would lead to a corrected age of 8116 ± 100 a cal B.P., close to the ~8000 a for the Unit II/III boundary of *Lamy et al.* [2006]. This is more reasonable because the entrance of marine Mediterranean water around 9.3 ka cal B.P. (see section 7.3) should have lowered the reservoir age of the Black Sea. The revised age model of GeoB 7608-1 was transferred to the other cores from the slope transect through detailed correlations using XRF and color scan data following the procedure described by *Bahr et al.* [2005].

[15] In addition to the reservoir age changing with time, water masses from shallow depth (i.e., above ~400 m) seem to diverge with respect to their reservoir age from those in greater depths with the beginning of the Bølling warm period [*Kwiecien et al.*, 2008]. This differs from earlier assumptions

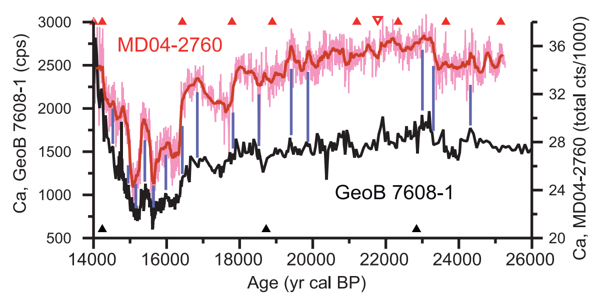

Figure 2. The glacial part of core GeoB 7608-1 tuned to MD04-2760 using XRF-scanning data (Ca is shown in counts per second for GeoB 7608-1 and total counts for MD04-2760 with a 21-point running average). The red triangles indicate the age control points for MD04-2760 [*Kwiecien et al.*, 2008]; the Y-2 tephra is indicated by an open triangle; and the black triangles are the radiocarbon dates made on GeoB 7608-1. Blue lines visualize tie-points between both Ca records (for optical reasons, not all tie-points were shown for the interval 16 to 14 ka cal B.P.).

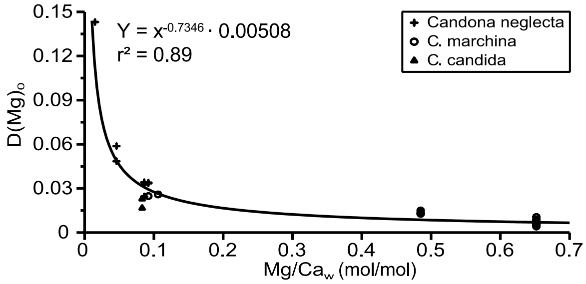

Figure 3. Relationship of the partition coefficient $D(Mg)_o$ of *Candona neglecta*, *C. marchina*, and *C. candida* to the host water Mg/Ca_w [after *Wansard et al.*, 1998]. The best fit ($r^2 = 0.89$) is represented by the function $D(Mg)_o = (Mg/Ca_w)^{-0.73} \cdot 0.0051$.

where an age offset between shallow and deep water has been proposed also for the pre-Bølling [*Bahr et al.*, 2005]. Further details on the potential mechanisms for the reservoir age evolution in the Black Sea are thoroughly discussed by *Kwiecien et al.* [2008].

5. Factors Influencing the Sr/Ca and Mg/Ca Ratios in Ostracod Shells

[16] Since the pioneering work in the early 1980s [*Chivas et al.*, 1983], many studies were performed to decipher the processes governing the uptake of trace and minor elements (especially Sr and Mg) into ostracod shells and to establish Mg/Ca and Sr/Ca records obtained on ostracod shells as powerful tools for reconstructing paleoenvironmental changes. Despite the steady increase in data from field and laboratory experiments, these studies had different conclusions regarding the influence of parameters like the host water's Sr/Ca and Mg/Ca ratios, Mg and Sr concentrations, temperature, pH or salinity on the ostracod shell chemistry. *Chivas et al.* [1985, 1986a, 1986b] first determined the dependence of the Mg/Ca and Sr/Ca of the ostracode shell (in the following termed Mg/Ca_o and Sr/Ca_o) on the Mg/Ca and Sr/Ca ratio of the host waters (Mg/Ca_w and Sr/Ca_w). The uptake of Sr and Mg relative to Ca into the ostracod shell is controlled by the partition coefficient $D(M)_o$ (M stands for either Sr or Mg) that is defined as

$$D(M)_o = (M/Ca_o)/(M/Ca_w).$$

[17] These authors also stated that $D(M)_o$ is the same for species belonging to the same genus and for closely related genera. This view was later contested claiming that the effect of Mg/Ca_w on Mg/Ca_o is minor and temperature is the controlling factor on Mg/Ca_o [*Palacios-Fest and Dettman*, 2001]. This point was also addressed by a study incorporating different species belonging to the genus *Candona* [*Wansard et al.*, 1998] which showed an important influence of Mg/Ca_w on $D(Mg)_o$: $D(Mg)_o$ is nearly constant above a Mg/Ca_w of ~0.1 mol/mol but increases exponentially below this threshold (Figure 3). This behavior of $D(Mg)_o$ especially affects the very low (<0.1 mol/mol) Mg/Ca_w values estimated by the measured Mg/Ca_o ratios in the glacial part of our records (see section 7.1).

[18] The temperature dependence of Mg/Ca_o (with probable exceptions [*Wansard et al.*, 1999]) has so far predominantly been used for temperature reconstructions in the marine realm [e.g., *Dwyer et al.*, 1995; *Ingram*, 1998]. Reconstructions in mesohaline or freshwater conditions were performed in fewer cases [*Wansard*, 1996; *Wansard and Roca*, 1997; *Palacios-Fest et al.*, 2002; *Cronin et al.*, 2003]. Temperature reconstructions on lakes are complicated by the variability of Mg/Ca_w due to evaporation and the precipitation of different mineral phases while Mg/Ca_w in the ocean remains more or less constant on longer timescales. *Engstrom and Nelson* [1991] did a temperature calibration for the species *Candona rawsoni* and obtained the relation $T = (Mg/Ca_o - 0.004)/(Mg/Ca_w \cdot 0.0000968)$. Although later studies suggested that *C. rawsoni* might not belong to the genus *Candona*, one can assume that the temperature sensitivity of Candonids lies in the range of that observed within other genera, i.e., a rise of 1 mmol/mol Mg/Ca equals a temperature increase of 1–2°C [*Wansard*, 1996; *De Deckker et al.*, 1999; *Müller*, 1999; *Palacios-Fest and Dettman*, 2001; *Cronin et al.*, 2003]. There were also suggestions that $D(Sr_o)$ is dependent on temperature [*De Deckker et al.*, 1999; *Majoran et al.*, 1999; *Müller*, 1999]. *Müller* [1999] proposed that organisms building shells with a higher Sr/Ca_o ratio are generally showing a higher sensitivity of $D(Sr)_o$ toward temperature, while the temperature-dependence of Mg/Ca_o decreases simultaneously. This might help to explain why for some ostracods (e.g., *Cyprideis australensis* [*De Deckker et al.*, 1999]) a temperature-dependent partitioning of strontium was described, but for others (e.g., *Candona* [*Wansard et al.*, 1998]) not.

[19] Even though there are apparent uncertainties about the interspecific or even intraspecific variability of factors controlling the Mg and Sr uptake, it seems appropriate to apply the results obtained

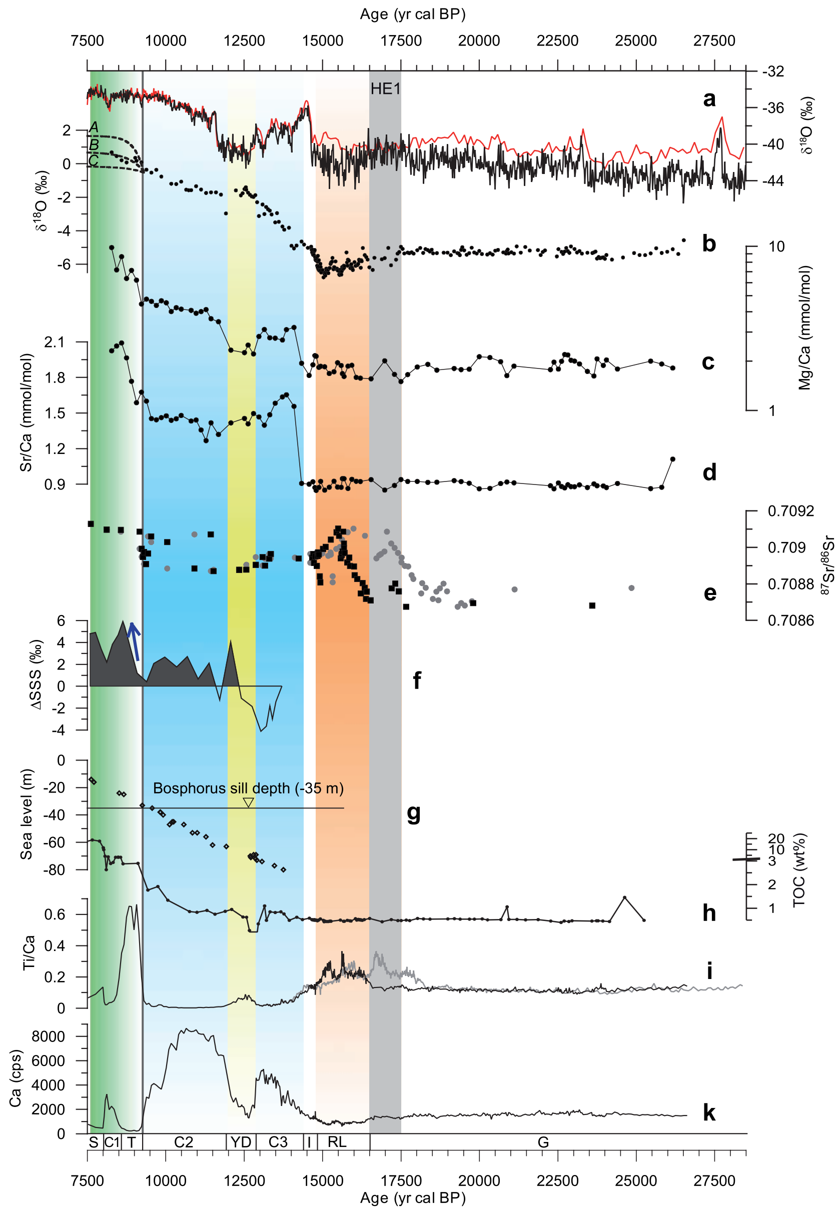

Figure 4. Comparison of the (a) Greenland NGRIP (black, GICC05 chronology [*Rasmussen et al.*, 2006; *Vinther et al.*, 2006; *Andersen et al.*, 2006]) and GISP2 (red, [*Grootes and Stuiver*, 1997]) ice core records with (b) stable oxygen isotopes of GeoB 7608-1 ($\delta^{18}O$) [*Bahr et al.*, 2006], (c) Mg/Ca (on logarithmic scale), and (d) Sr/Ca of *Candona schweyeri* from core GeoB 7608-1. (e) Compilation of $^{87}Sr/^{86}Sr$ measurements on ostracod and bivalve shells from 18 different cores in the western Black Sea continental slope and shelf [*Major et al.*, 2006]. The grey squares are the values plotted using the stratigraphy from *Major et al.* [2006]. Black squares those tuned to the present record. (f) Salinity record from the Sea of Marmara compared to modern [*Sperling et al.*, 2003]. (g) Global sea level record from Tahiti [*Bard et al.*, 1996] and the present sill depth of the Bosphorus. (h) Total organic carbon (TOC) of GeoB 7608-1 (please note the break in the scale of the axis). (i) XRF Ti/Ca of GeoB 7608-1 in the present stratigraphy (black line) and Ti/Ca applying the stratigraphy used by *Bahr et al.* [2006] (grey line) and (k) XRF Ca record from GeoB 7608-1 [*Bahr et al.*, 2005]. Indicated are the different lithological sections: S, sapropel; C1–C3, periods of authigenic carbonate precipitation (blue bars), interrupted by dominant clastic sedimentation during "T" (transition, start of marine inflow; S, C1, and T are combined shown as a green bar) and "YD" (Younger Dryas, yellow bar); I, interval between C3 and RL, red clay layers (red bar); G, glacial part prior to ~16.5 ka B.P. Dashed lines in Figure 4b indicate the hypothetical $\delta^{18}O$ evolution of Black Sea water for a maximum flux (5475 km^3/a), a moderate flux (500 km^3/a), and a small inflow (80 km^3/a) of Mediterranean/Sea of Marmara water through the Bosphorus into the Black Sea. HE1, Heinrich Event 1. Note that the timing of HE1 was chosen according to *Rinterknecht et al.* [2006]; see also discussion (section 7.1).

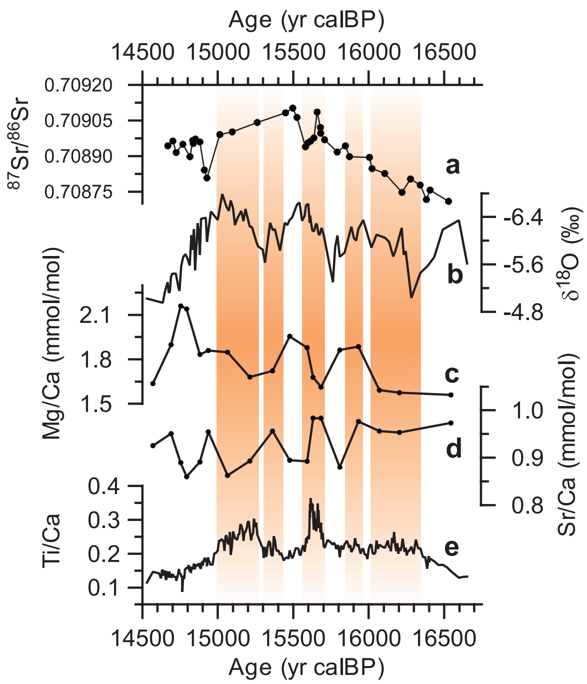

Figure 5. Focus on the period of red clay layer deposition: (a) $^{87}Sr/^{86}Sr$ measurements on ostracods and bivalves from *Major et al.* [2006]; (b) $\delta^{18}O$ [*Bahr et al.*, 2006] of *Candona spp.*, (c) Mg/Ca and (d) Sr/Ca of *Candona schweyeri* from GeoB 7608-1; and (e) Ti/Ca ratio from GeoB 7608-1 [*Bahr et al.*, 2005]. Red bars indicate periods of maximum terrigenous input (high Ti/Ca ratio).

by *Wansard et al.* [1998] to our record, i.e., $D(Mg)_o$ is dependent on Mg/Ca_w and temperature, whereas Sr/Ca_o only depends on Sr/Ca_w. *Wansard et al.*'s [1998] study is based on a broad spectrum of *Candona* species that all yielded consistent results [*Wansard et al.*, 1998]. Another important point is that the hydrological conditions in the ancient Black Sea (low salinity; low Mg/Ca_w and Sr/Ca_w, see section 7.1) are similar to the environments investigated by *Wansard et al.* [1998].

6. Results

[20] The glacial period until ~16.5 ka B.P. ("G" in Figure 4) exhibits only low variability in all records with low TOC values around 0.5 wt% (with two probable outliers). The first distinct change occurred between 16.5 and 14.8 ka B.P. where consecutive drops in $\delta^{18}O$ are recorded. This period is marked by a series of reddish-brown clay layers ("RL," Figures 4 and 5) in the western Black Sea, characterized by increased concentrations of terrigenous elements [*Bahr et al.*, 2005] and anomalous high illite and kaolinite contents [*Major et al.*, 2002]. During this interval, an increase in $^{87}Sr/^{86}Sr$ from Last Glacial Maximum (LGM)-values around 0.70870 to 0.70910 is recorded. Note, that the $^{87}Sr/^{86}Sr$ record by *Major et al.* [2006] was tuned to the new stratigraphy using the red layer interval and the Ca peaks as an independent time marker (Figure 4e).

[21] After 14.8 ka B.P. $^{87}Sr/^{86}Sr$ values drop to ~0.70896, while $\delta^{18}O$ has a trend toward higher values, only interrupted by a relatively constant interval during the Younger Dryas ("YD"). The overall $\delta^{18}O$ shift totals approximately +7.2‰ (from approximately −6.5‰ at 14.8 ka B.P. to +0.7‰ at 8.0 ka B.P.).

[22] Mg/Ca and Sr/Ca both increase dramatically at 14.5 ka B.P.: Mg/Ca from 1.6 to 3.2 mmol/mol; Sr/Ca from 0.9 initially to 1.65 mmol/mol, later decreasing to 1.45 mmol/mol. The change in the Mg/Ca and Sr/Ca ratios at 14.5 ka B.P. coincides with the precipitation of calcite which lasts from 14.5 to 7.5 ka B.P. (Ca peaks "C1"–"C3" in Figure 4k), interrupted by two periods of dominant clastic deposition during the YD and around 8.5 ka B.P. ("YD" and "T," Figure 4). $^{87}Sr/^{86}Sr$ values remain constant until circa 12.8 ka B.P. where it drops to 0.70888. At circa 9.3 ka B.P. (beginning of stage "T") Mg/Ca and Sr/Ca ratios and strontium isotopes show a final increase to maximum values. With the onset of calcite peak "C3" the TOC content starts to increase steadily to reach values of up to 1.1 wt%, drops at the beginning of the YD interval to 0.34 wt% and then increases again to around 3 wt% at stage "T." Afterward it rises sharply to a maximum of 22.3 wt% in the sapropel.

[23] Although both, Mg/Ca and Sr/Ca, seem to covary along the record at the first glance, they do show some distinct differences, e.g., the low in Mg/Ca during the YD that is not mirrored in Sr/Ca, and the constant Sr/Ca level in the early Holocene is accompanied by a slight but steady increase in Mg/Ca.

[24] As shown in Figure 6, most of the values taken from the cores along the slope transect are in the same range. Exceptions are the measurements taken from the shallow core GeoB 7610-1. The Mg/Ca values of core GeoB 7610-1 are constantly higher until 10.5 ka B.P., while Sr/Ca slightly increases between 12.5 and 10 ka B.P. Mg/Ca measurements obtained on GeoB 7604-2 are also

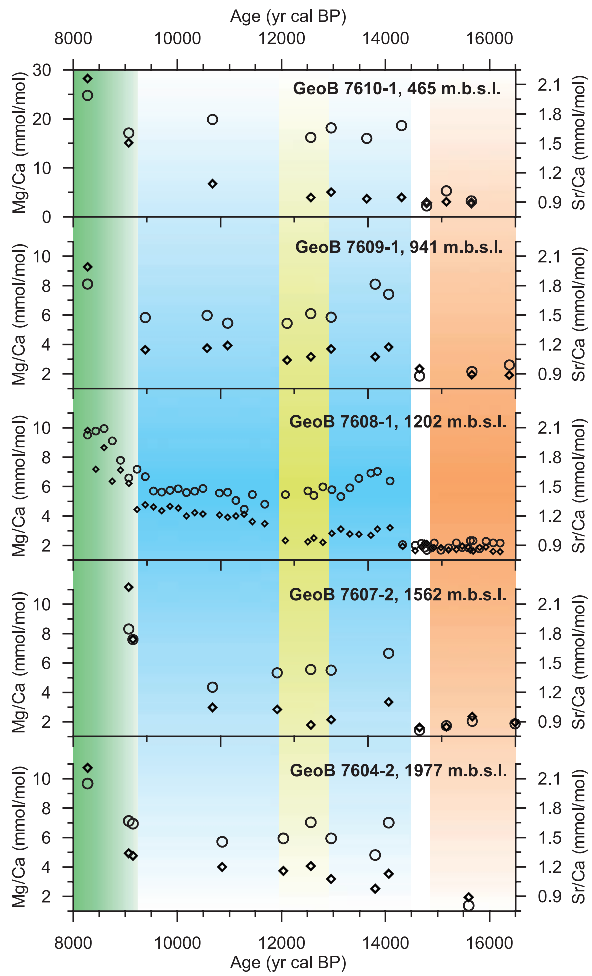

Figure 6. Comparison of Mg/Ca (diamonds) and Sr/Ca (circles) data of *Candona schweyeri* from different depths in the northwestern Black Sea. Core name and water depth in meters below sea level (m.b.s.l.) are given. Note that the scale for Mg/Ca of GeoB 7610-1 is different from the other. Colored bars mark the red clay layer interval (red), Ca peaks (blue), Younger Dryas (yellow), and inflow of Mediterranean waters (green).

higher than those of the shallower cores during the YD.

7. Interpretation and Discussion

[25] Although $\delta^{18}O$ is a widely used parameter in paleo studies, results and interpretations based on this proxy alone can be ambiguous, because it depends on numerous factors such as water temperature, evaporation, isotopic composition of runoff, and precipitation. With the additional use of Mg/Ca and Sr/Ca it is possible to further constrain the factors influencing $\delta^{18}O$, since Mg/Ca is temperature dependent and both Mg/Ca and Sr/Ca give insight into changes of the water chemistry. A major focus of our study is the timing of the reconnection of the Black Sea with the Mediterranean Sea via the Sea of Marmara. In this context, $^{87}Sr/^{86}Sr$ ratios give valuable results, because ocean water and fresh or slightly brackish lake water have distinctly different isotopic composition [see also *Major et al.*, 2006]. Since the $\delta^{18}O$ and $^{87}Sr/^{86}Sr$ records have been published and discussed elsewhere ($^{87}Sr/^{86}Sr$ by *Major et al.* [2006]; $\delta^{18}O$ by *Bahr et al.* [2006]) we focus on the Mg/Ca and Sr/Ca records.

[26] Mg/Ca and Sr/Ca values measured on sediment core GeoB 7608-1 are generally positively correlated (Figures 4 and 7) and therefore suggest a common controlling factor. However, a closer inspection shows that the Mg/Ca_o and Sr/Ca_o values group into well-defined clusters (Figure 7) that are related to the stratigraphic subdivision presented in Figure 4. Hence we must assume that in each of these periods different environmental conditions affected the Mg/Ca and Sr/Ca ratios found in the ostracod shells. In the following discussion we will first examine the glacial con-

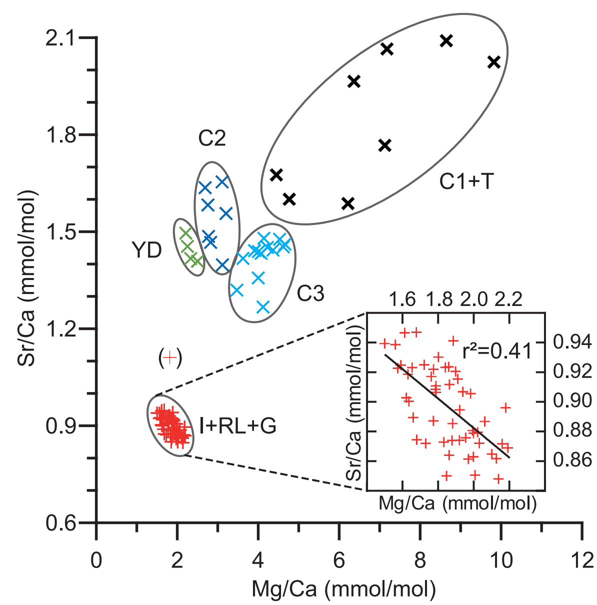

Figure 7. Correlation of Mg/Ca and Sr/Ca measurements on ostracods from core GeoB 7608-1. The small inset shows an augmentation of this anticorrelation for the period before 14.5 ka B.P., with a potential linear fit (r^2 = 0.41) of Sr/Ca = –0.100 · Mg/Ca + 1.081. Circles denote the clustering of the measurements into groups that follow the lithological sections presented in Figure 4. The measurement in brackets represents the oldest sample from the glacial ("G") part, plotting outside the "I + RL + G" group.

ditions until 14.5 ka B.P., then the periods of the late glacial to early Holocene, and finally we focus on the inflow of Mediterranean waters around 9.3 ka B.P.

7.1. Glacial Conditions

[27] Sr/Ca and Mg/Ca are constantly on a very low level until 14.5 ka B.P. (Figure 4, cluster "I + RL + G" in Figure 7), implying stable environmental and hydrologic conditions throughout this time. Low Sr/Ca, Mg/Ca, $\delta^{18}O$ and $^{87}Sr/^{86}Sr$ values generally indicate fresh or slightly brackish conditions as also suggested by faunal investigations [*Mudie et al.*, 2002a]. A Sr/Ca_w ratio of 2.70 ± 0.08 mmol/mol for the glacial Black Sea water could be calculated using the obtained Sr/Ca_o values and the published $D(Sr)_o$ of 0.332 for *Candona neglecta* and *C. marchina* [*Wansard et al.*, 1998]. 2.70 mmol/mol is higher than the average Sr/Ca_w of 2.20 mmol/mol for river water entering the Black Sea [*Major et al.*, 2006], indicating that either the partition coefficient of *Candona schweyeri* is higher than assumed for other Candonids (the $D(Sr)_o$ of *C. schweyeri* would be 0.408 in this case) or the Sr/Ca_w ratio of the glacial water was enriched relative to the calculated mean river input. Interestingly, *Major et al.* [2006] also calculated an unusually high D(Sr) for their Sr/Ca measurements on bivalve shells in the same time period, which might be coincidental, but could also indicate that Sr/Ca_w was higher than expected, fitting to assumptions that the glacial "Black Lake" was not fully fresh [*Mudie et al.*, 2002a] but enriched relative to the river composition because of evaporation.

[28] Using the range of the $D(Mg)_o$ shown in Figure 3 (approximately 0.015 to 0.15) and a Mg/Ca_o of 0.002 mol/mol yields low Mg/Ca_w values between 0.013 to 0.13 mol/mol. This indicates on one hand side freshwater conditions, but also strengthens the point that the variations in Mg/Ca_o are effected by the strong exponential gradient in $D(Mg)_o$ for Mg/Ca_w values <0.1 mol/mol (Figure 3; see also section 5).

[29] The entrance of isotopically depleted water between 16.5 and 14.8 ka B.P. causes a drop in $\delta^{18}O$ [*Bahr et al.*, 2006] ("RL" in Figure 4). The observed high $^{87}Sr/^{86}Sr$ values [*Major et al.*, 2006] and the abundance of illite and kaolinite typical for a northern sediment source [*Major et al.*, 2002] indicate that an otherwise unimportant or inactive region contributed to a considerable extent to the sediment and water input during this time. As one of the potential sources for the incoming water the Caspian Sea has been proposed [e.g., *Major et al.*, 2002; *Ryan et al.*, 2003; *Bahr et al.*, 2005], which might have spilled into the Black Sea via the Manych Depression during periods of high lake level. The timing of the highest lake level in the Caspian Sea during the late Pleistocene is subject of debate, but the present estimates suggest that it occurred either earlier than the red layer deposition at $\sim$18 ka cal B.P. [*Kroonenberg et al.*, 1997; *Svitoch*, 1999] or later around 12 ka cal B.P. [*Svitoch*, 2007]. Thus a Caspian source cannot be excluded, but remains speculative [see also *Major et al.*, 2006]. As an alternative, *Bahr et al.* [2006] proposed that meltwater from the FIS might have caused the red layer deposition. However, this is unlikely since recent studies showed that the meltwater discharge was directed toward the Baltic Sea or farther west to the Bay of Biscay [*Ménot et al.*, 2006] and the Arctic Ocean in the north [*Demidov et al.*, 2006; *Ménot et al.*, 2006]. Interestingly it has been noted that after Heinrich Event 1 and before the warming of the Bølling, a re-advance of alpine glaciers (Gschnitz stadial) and of the FIS (Pomeranian moraine) was observed, contemporaneous to the deposition of the red layers. The paleoclimatic interpretations are contradictory, in the case of the Gschnitz stadial it was argued that extremely cold and arid conditions were prevailing [*Ivy-Ochs et al.*, 2006], while *Rinterknecht et al.* [2006] propose that the extremely arid conditions were restricted to Heinrich Event 1 (HE1) dated to circa 17.5–16.5 ka B.P. in the continental chronology used by *Rinterknecht et al.* [2006]. Note that HE1 sensu strictu is related to the occurrence of detrital dolomitic carbonate grains originated from the Laurentide Ice Sheet, occurring circa 15.5–16 ka B.P. in the eastern Atlantic [*Knutz et al.*, 2007], but with several HE-precursors of ice-rafted debris originating from the European continent (British Ice Sheet and FIS) starting at circa 18 ka B.P. [*Knutz et al.*, 2007]. *Rinterknecht et al.* [2006] explain the observed advance of the southern margin of the Scandinavian Ice Sheet shortly before the Bølling with a slightly increased precipitation. A more positive hydrological balance might therefore account for an higher inflow of isotopically depleted water from the northern drainage area (via Dnestr and Dnepr) where the frozen soils increased the surface runoff. A dominant contribution from the alpine region is unlikely since the distinct signals of the XRF-element composition, clay mineralogy [*Major et al.*, 2002] and $^{87}Sr/^{86}Sr$ ratio of ostracod shells [*Major et al.*, 2006] point to a water/sediment source with char-

acteristics considerably different from the water/sediment supplied by the Danube, which is otherwise exerting the dominant influence on the study sites in the NW Black Sea.

[30] In contrast to $^{87}Sr/^{86}Sr$, both Mg/Ca and Sr/Ca, remain on the same level as before (Figure 7), which indicates that the incoming water had Mg/Ca and Sr/Ca ratios relatively similar to that of the glacial Black Sea. The decrease of the strontium isotope ratio after the water inflow points to an outflow of the Black Sea into the Sea of Marmara: the ^{87}Sr-rich lake water would leave the Black Sea to be replaced by more ^{87}Sr depleted river water until the water balance turned negative and the Black Sea lake level dropped below the Bosphorus sill depth.

[31] Although there is no significant correlation between the Mg/Ca and Sr/Ca records compared to the $\delta^{18}O$ or the XRF Ti/Ca ratio, the Mg/Ca and Sr/Ca ratios are to some extent inversely correlated during the glacial, especially during the red layer period (Figure 5 and inset in Figure 7). One possible reason could be that a slight warming (increased Mg/Ca_o) was accompanied by the input of slightly Sr/Ca-depleted water from the northern drainage area (Figure 5). Compared to the full range of the climatic fluctuations one can expect that the amplitude of the temperature variability in the deeper part of the Black Sea should be reduced. If we apply the temperature estimates discussed in section 5 to the Mg/Ca ratio, a variability of ~0.5 mmol/mol Mg/Ca_o during the red layer period might be translated into temperature fluctuations of ~0.5 to 1°C in the Black Sea at 1200 m depth, however, given the sensitivity of this method and the probable influence of other factors on the Mg/Ca_o this has to be viewed with caution.

7.2. Conditions After 14.5 ka B.P.

[32] Both Sr/Ca and Mg/Ca records from GeoB 7608-1 show a drastic shift at 14.5 ka B.P., with the onset of the B/A warm period (Figure 4). Since Sr/Ca and Mg/Ca are sensitive to changes in the water chemistry, it is reasonable to assume a relationship to the contemporaneous onset of calcite precipitation in the surface water, mirrored, e.g., in the Ca record (Figure 4). The calcite precipitation is most likely caused by the assimilation of CO_2 in the surface water through increased phytoplankton activity during favorable climatic conditions, as corroborated by increasing TOC values with the onset of the B/A, indicating enhanced primary productivity (Figure 4h). The uptake of Sr and Mg relative to Ca into the precipitated calcite (organic and inorganic) is controlled by the partition coefficient $D(M)_c$ that is defined similarly to the partition coefficient that governs the uptake of Sr and Mg into the ostracod shell [*Morse and Bender*, 1990]:

$$D(M)_c = (M/Ca_c)/(M/Ca_w)$$

where M is either Sr or Mg.

[33] Numerous attempts to quantify $D(Sr)_c$ and $D(Mg)_c$ for inorganic calcite [e.g., *Howson et al.*, 1987; *Morse and Bender*, 1990; *Burton and Walter*, 1991] have shown that especially $D(Mg)_c$ is governed by a complex interaction of several parameters, including temperature, Mg/Ca_w, the Mg-concentration of the ambient water, P_{CO2}, and the calcite precipitation rate [e.g., *Huang and Fairchild*, 2001]. For conditions that come close to the ancient Black Sea with low salinity and low to moderate alkalinity, the $D(Mg)_c$ for inorganic low-Mg calcite has been calculated to be in the range of 0.031 (for 25°C), 0.019 (15°C), and 0.012 (6.6°C) [*Huang and Fairchild*, 2001]. The same study gives $D(Sr)_c$ values between 0.057–0.078. As these values are below 1.0, precipitating calcite would therefore be depleted in Sr and Mg relative to Ca and the upper water column would remain enriched in Sr and Mg. The data suggests that after an initial phase with overshooting Sr/Ca_w a chemical equilibrium was reached lasting until the final increase of Sr/Ca_w and Mg/Ca_w at 9.3 ka B.P.. Similar trends are also reported in the bivalve Sr/Ca record by *Major et al.* [2006] (Figure 4e), with the difference that Sr/Ca almost returns to LGM values after the initial increase at 14.5 ka B.P.. However, there is a considerable scatter in this record, probably due to the fact that the sampled cores are located in different water depths (49–378 m) and the thermodynamically unstable aragonite of the bivalve shells might be more affected by diagenetic alterations than the low-Mg-calcite carapaces of the ostracod.

[34] An important question is if the Mg/Ca_o increase at 14.5 ka B.P. is caused exclusively by the described changes in the water chemistry, or if temperature changes add to the observed signal. The abrupt B/A warming is well documented from other regions (e.g., central Europe [*Friedrich et al.*, 2001], Sea of Marmara [*Mudie et al.*, 2002b]), and it seems therefore likely that the Black Sea experienced a significant warming as well. Decreasing temperatures certainly play a role for the Mg/Ca_o

decrease during the YD, because if changes in the water chemistry would be responsible only, Mg/Ca_o and Sr/Ca_o would parallel each other. This is apparently not the case, except for GeoB 7604-2, which is discussed later. The observed drop of 1 mmol/mol in Mg/Ca_o in GeoB 7608-1 equals a temperature decrease of 1–2°C and explains the slightly increased $\delta^{18}O$ during the YD. If only governed by the change in the isotopic composition of the meteoric precipitation [*Bahr et al.*, 2006], the oxygen isotope data would show a drop rather than an increase, because the $\delta^{18}O$ of meteoric almost reached its LGM-level during the YD [*von Grafenstein et al.*, 1999a]. With the evidence of a cooling during the YD, a preceding temperature increase during the B/A seems very reasonable. After the rapid temperature increase following the termination of the YD, a slight but continuous warming of the intermediate water column over the course of the early Holocene also explains the 1 mmol/mol increase of Mg/Ca_o at constant Sr/Ca_o values between 11.5 and 9.5 ka B.P. The influence of temperature on Mg/Ca_o might therefore discriminate the periods “C3,” “YD” and “C2” into the different clusters shown in Figure 7 (note that these clusters are mainly separated by different Mg/Ca_o values, while the respective Sr/Ca_o ratios are not distinctly different).

[35] A possible stratification of the Black Sea water column during this time interval has already been discussed on the basis of the observation of diverging ostracod-$\delta^{18}O$ trends [*Bahr et al.*, 2006]. The overall increase in $\delta^{18}O$ since ~15 ka B.P. is, at least for the B/A, mainly caused by increased $\delta^{18}O$ in the atmospheric precipitation and runoff. Nevertheless, $\delta^{18}O$ values are enriched in the deep core GeoB 7604-2 (1977 m water depth) between 14.5 and 9.3 ka B.P., indicating that the deep water is separated to a certain extent from the intermediate water body [*Bahr et al.*, 2006]. There is, however, no significant difference in the Sr/Ca and Mg/Ca ratios for these depth levels (Figure 6). This is most likely due to the different factors influencing the $\delta^{18}O$ on one side and the Mg/Ca and Sr/Ca records on the other side: the diverging trend in $\delta^{18}O$ is probably controlled by the adjustment of the deepwater to increased $\delta^{18}O$ of atmospheric precipitation [*Bahr et al.*, 2006] that has no direct impact on the Mg/Ca or Sr/Ca record. An exception are Mg/Ca values from the deepest core GeoB 7604-2 that are higher than those in the intermediate cores during the YD, suggesting that the temperature drop during the YD did not affect the deep water. However, during the rest of the glacial/deglacial period temperatures seem to have been quite uniform in intermediate and deep water depths.

[36] In the previous section, the $^{87}Sr/^{86}Sr$ decrease after the red layer period was linked to an outflow of Black Sea water combined with changes in the freshwater sources; the same argument could be raised for the drop in the strontium isotope ratio to almost LGM levels during the YD. A positive water balance and therefore a high lake level during the YD (in opposition to a low level during B/A and early Holocene) have also been proposed by other authors on the basis of sedimentological, geochemical, and biological evidence [e.g., *Ryan et al.*, 2003; *Major et al.*, 2006].

7.3. Reconnection With the Mediterranean Sea

[37] The deglacial rise of the global sea level together with the present sill depth of the Bosphorus (−35 m) suggests that the inflow of Mediterranean water started between 9.5 and 9.0 ka B.P. (Figure 4). It has been argued that the Bosphorus sill might have been at least 7 m shallower before the breaching of the barrier [*Sperling et al.*, 2003], which would have postponed the inflow to about 8.7 ka B.P. The final increase of Sr/Ca_o and Mg/Ca_o in our record started at 9.3 ka B.P. (Figure 4, cluster “C1 + T” in Figure 7) and is unquestionably related to the intrusion of Mediterranean water with high Sr/Ca_w and Mg/Ca_w ratios. This also fits to the abrupt $^{87}Sr/^{86}Sr$-increase [*Major et al.*, 2006]. An additional point that supports the inflow of saline Mediterranean water at circa 9.0 ka B.P. are sea surface salinity (SSS) estimates from the Sea of Marmara [*Sperling et al.*, 2003]. This record shows a strong increase in SSS starting ~9 ka B.P. (Figure 4) that suggests an enhanced passage of high-salinity Mediterranean water through the Sea of Marmara during the flooding of the Black Sea.

[38] A similar question as for the 14.5 ka B.P. shift arises for the Sr/Ca and Mg/Ca increase after 9 ka B.P.: is there a temperature-component in the Mg/Ca_o signal beside the introduction of Mg and Sr-enriched Mediterranean water? The introduction of warm Mediterranean water could have increased the temperature in the deep Black Sea during this time, probably accompanied by turbulent mixing that led to a subsequent homogenization of the water column, as indicated by the similar values found for Mg/Ca, Sr/Ca and $\delta^{18}O$ in cores from different depth (Figure 6). An exception are the youngest two Mg/Ca measurement in 7610-1,

which are likely to be influenced by secondary high-magnesium calcite precipitating from methane-rich fluids that caused the formation of carbonate concretions in the overlying sapropel. Any attempt to calculate the temperature-component in the final Mg/Ca_o increase is hindered by the exponential relation of $D(Mg)_o$ to Mg/Ca_w. Furthermore, it has to be taken into account, that the process of mixing of the two end-members with different Mg/Ca_w and Sr/Ca_w ratios (Black Sea freshwater versus Mediterranean marine water) is nonlinear and the initial concentrations of Sr, Mg, and Ca in the water of the Black Sea are unknown [see, e.g., *Anadón et al.*, 2002].

[39] Despite these problems, the $\delta^{18}O$ record can be used to give a rough estimate on the volume flux during the reconnection with the Mediterranean Sea. A simple calculation with an isotopic balance model based on the program HIBAL [*Benson and Paillet*, 2002], modified to fit the conditions of the Black Sea [*Bahr et al.*, 2006], was performed to calculate the hypothetical evolution of the $\delta^{18}O$ of the Black Sea water (Figure 4b) during the inflow of Mediterranean water. $\delta^{18}O$ measurements obtained on the planktic foraminifera *Turborotalita quinqueloba* from the Sea of Marmara at 9.5 ka B.P. give an indication of the $\delta^{18}O$ of the inflowing water at that point of time. The values are around +1.2‰ [*Sperling et al.*, 2003], or ~3.32‰ for our record, if the vital offset of +2.2‰ for Candoninae [*von Grafenstein et al.*, 1999b] is taken into consideration. This yields an approximate $\delta^{18}O_{water}$ of +0.21‰ (calculated for 10°C water temperature) when using the formulas given by *von Grafenstein et al.* [2000]. For the Black Sea water a $\delta^{18}O$ value of −4.3‰ (for 8°C) was estimated from the ostracod-$\delta^{18}O$ at 9.3 ka B.P. The three scenarios shown in Figure 4b include a catastrophic inflow with the maximum possible flux thorough the Bosphorus (5475 $km^3\ a^{-1}$ [*Myers et al.*, 2003]), a reduced inflow of 500 $km^3\ a^{-1}$, being equal to roughly the half of the combined amount of water (900 $km^3\ a^{-1}$ [*Öszoy and Ünlüata*, 1997]) flowing presently in both directions through the Bosphorus, and a very low flux of 80 $km^3\ a^{-1}$. Although the boundary conditions of the calculations are debatable, $\delta^{18}O$ is not in steady state at the point at 9.3 ka B.P. ($\delta^{18}O$ is not constant) and the simulation makes use of very simplifying assumptions (full mixing, constant inflow, steady water temperatures), it shows that a fast inflow would leave a clear signal in the $\delta^{18}O$ record (Figure 4b). On the other hand, a very low inflow would not change the $\delta^{18}O$ values considerably. Since the best fit is reached with 500 $km^3\ a^{-1}$, the volume flux of the inflow seems to be in between these extremes. Thus, if we expect a volume in the order of 40,000 km^3 to be filled [*Myers et al.*, 2003] the flooding would last ~100 a, longer than the 2–3 a implied by the original "catastrophic flooding" scenario [*Ryan et al.*, 1997], but in geological timescales still fairly short.

8. Conclusion

[40] Sr/Ca, Mg/Ca, $\delta^{18}O$ and $^{87}Sr/^{86}Sr$ records obtained on ostracod valves reveal major changes in the Black Sea hydrochemistry from the Last Glacial Maximum to the early Holocene, driven by climatic and hydrological fluctuations. Prior to 16.5 ka B.P., the records show little variability and thus constant environmental conditions. Between 16.5 and 14.8 ka B.P., a series of water pulses presumably from a northern source led to the temporal depletion of the stable isotopic composition of the Black Sea water and to a significant, source-related increase in the $^{87}Sr/^{86}Sr$ ratio. At 14.5 ka B.P. major shifts in the water chemistry took place, related to the onset of the Bølling/Allerød warm period. While the $\delta^{18}O$ values are gradually increasing due to the influence of isotopically enriched atmospheric precipitation and runoff, the Sr/Ca and Mg/Ca ratios are abruptly shifting to higher values, caused by the precipitation of authigenic calcite during high phytoplankton productivity, and the associated increase in Mg and Sr concentrations in the water column. During the Younger Dryas cold period low Mg/Ca values indicate a drop of 1–2°C in the deep water, accompanied by an interruption of the calcite precipitation in the surface water due to high phytoplankton activity. A potential outflow of the Black Sea during this time is implied by the decreasing $^{87}Sr/^{86}Sr$ values. The reconnection of the Black Sea with the Mediterranean Sea via the Sea of Marmara started at 9.3 ka B.P. as marked in an increase in the Mg/Ca, Sr/Ca and $^{87}Sr/^{86}Sr$ ratios. Modeling of the $\delta^{18}O$ record indicates that it needed nearly 100 a until global and Black Sea level were adjusted.

Acknowledgments

[41] We thank captain and crew of the R/V *Meteor* for their support during the Meteor cruise M 51-4. We also gratefully acknowledge Scott Birdwhistell for running the ICP-MS at WHOI, Monika Segl (University Bremen) and her team for doing the stable isotope measurements, and Ursula Röhl (University Bremen) for support of the XRF measurements.

Bernhard Schnetger (ICBM, Oldenburg) kindly provided unpublished TOC data. A stay of A.B. at the WHOI was supported by the DAAD (ref. D/04/42992). This research was funded by the DFG grants LA 1273/2-1, LA 1273/2, and WE 992/47-3. RCOM 0517.

References

Aksu, A. E., R. N. Hiscott, D. Yasar, F. I. Isler, and S. Marsh (2002), Seismic stratigraphy of Late Quaternary deposits from the southwestern Black Sea shelf: Evidence for non-catastrophic variations in sea-level during the last ∼10000 yr, *Mar. Geol.*, *190*, 61–94.

Aloisi, G., M. Drews, K. Wallmann, and G. Bohrmann (2004), Fluid expulsion from the Dvurechenskii mud volcano (Black Sea): Part I. Fluid sources and relevance to Li, B, Sr, I and dissolved inorganic nitrogen cycles, *Earth Planet. Sci. Lett.*, *225*(3–4), 347–363.

Anadón, P., E. Gliozzi, and I. Mazzini (2002), Paleoenvironmental reconstruction of marginal marine environments from combined paleoecological and geochemical analyses on ostracods, in *Ostracoda: Applications in Quaternary Research*, *Geopyhs. Monogr. Ser.*, vol. 113, edited by J. A. Holmes, pp. 227–247, AGU, Washington, D. C.

Andersen, K. K., et al. (2006), The Greenland Ice Core Chronology 2005, 15–42 ka. Part 1: Constructing the time scale, *Quat. Sci. Rev.*, *25*(23–24), 3246–3257.

Bahr, A., F. Lamy, H. Arz, H. Kuhlmann, and G. Wefer (2005), Late glacial to Holocene climate and sedimentation history in the NW Black Sea, *Mar. Geol.*, *214*, 309–322.

Bahr, A., H. Arz, F. Lamy, and G. Wefer (2006), Late glacial to Holocene paleoenvironmental evolution of the Black Sea reconstructed with stable oxygen isotope records obtained on ostracod shells, *Earth Planet. Sci. Lett.*, *241*(3–4), 863–875.

Bard, E., B. Hamelin, M. Arnold, L. Montaggioni, G. Cabioch, G. Faure, and F. Rougerie (1996), Sea level record from Tahiti corals and the timing of deglacial meltwater discharge, *Nature*, *382*, 241–244.

Benson, L., and F. Paillet (2002), HIBAL: A hydrologic-isotopic-balance model for application to paleolake systems*Quat. Sci. Rev.*, *21*(12–13), 1521–1539.

Burton, E. A., and L. M. Walter (1991), The effects of PCO_2 and temperature on magnesium incorporation in calcite in seawater and $MgCl_2–CaCl_2$ solutions, *Geochim. Cosmochim. Acta*, *55*(3), 777–785.

Chester, R. (1990), *Marine Geochemistry*, 698 pp., Unwyn Hyman, London.

Chivas, A. R., P. De Deckker, and J. M. G. Shelley (1983), Magnesium, strontium and barium partitioning in nonmarine ostracod shells and their use in paleoenvironmental reconstructions—A preliminary study, in *Applications of Ostracoda*, edited by R. F. Maddocks, pp. 238–249, Univ. of Houston Geosci., Houston, Tex.

Chivas, A. R., P. De Deckker, and J. M. G. Shelly (1985), Strontium content of ostracods indicates lacustrine palaeosalinity, *Nature*, *316*, 251–253.

Chivas, A. R., P. De Deckker, and J. M. G. Shelley (1986a), Magnesium and strontium in non-marine ostracod shells as indicators of palaeosalinity and palaeotemperature, *Hydrobiologia*, *143*, 135–142.

Chivas, A. R., P. De Deckker, and J. M. G. Shelly (1986b), Magnesium content of non-marine ostracod shells: A new palaeosalinometer and palaeothermometer, *Palaeogeogr. Palaeoclimatol. Palaeoecol.*, *54*, 43–61.

Cronin, T. M., G. S. Dwyer, T. Kamiya, S. Schwede, and D. A. Willard (2003), Medieval Warm Period, Little Ice Age and 20th century temperature variability from Chesapeake Bay, *Global Planet. Change*, *36*(1–2), 17–29.

De Deckker, P., A. R. Chivas, and J. M. G. Shelley (1999), Uptake of Mg and Sr in the euryhaline ostracod Cyprideis determined from in vitro experiments, *Palaeogeogr. Palaeoclimatol. Palaeoecol.*, *148*, 105–116.

Demidov, I., M. Houmark-Nielsen, K. Kjær, and E. Larsen (2006), The last Scandinavian Ice Sheet in northwestern Russia: Ice flow patterns and decay dynamics, *Boreas*, *35*(3), 425–443.

Dwyer, G. S., T. M. Cronin, A. R. Baker, M. E. Raymo, J. S. Buzas, and T. Corrège (1995), North Atlantic deepwater temperature change during late Pliocene and late Quaternary climate cycles, *Science*, *270*, 1347–1351.

Engstrom, D. R., and S. Nelson (1991), Paleosalinity from trace metals in fossil ostracodes compared with observational records at Devils Lake, North Dakota, *Palaeogeogr. Palaeoclimatol. Palaeoecol.*, *83*, 295–312.

Eriksen, U., W. L. Friedrich, B. Buchardt, H. Tauber, and M. S. Thomson (1990), The Stronghyle Caldera: Geological, palaeontological and stable isotope evidence from radiocarbon dated stromatolites from Santorini, in *Thera and the Aegean World III*, vol. 2, *Earth Sciences*, edited by D. A. Hardy et al., pp. 139–150, Thera Found., London.

Friedrich, M., B. Kromer, K. F. Kaiser, M. Spurk, K. A. Hughen, and S. J. Johnsen (2001), High-resolution climate signals in the Bolling-Allerod Interstadial (Greenland Interstadial 1) as reflected in European tree-ring chronologies compared to marine varves and ice-core records, *Quat. Sci. Rev.*, *20*(11), 1223–1232.

Grootes, P. M., and M. Stuiver (1997), Oxygen 18/16 variability in Greenland snow and ice with 10^{-3}- to 10^{5}-year time resolution, *J. Geophys. Res.*, *102*(C12), 26,455–26,470.

Howson, M. R., A. D. Pethybridge, and W. A. House (1987), Synthesis and distribution coefficient of low-magnesium calcites, *Chem. Geol.*, *64*(1–2), 79–87.

Huang, Y., and I. J. Fairchild (2001), Partitioning of Sr^{2+} and Mg^{2+} into calcite under karst-analogue experimental conditions, *Geochim. Cosmochim. Acta*, *65*(1), 47–62.

Ingram, C. (1998), Palaeoecology and geochemistry of shallow marine ostracoda from the Sand Hole formation, Inner Silver Pit, southern North Sea, *Quat. Sci. Rev.*, *17*, 913–929.

Ivy-Ochs, S., H. Kerschner, P. W. Kubik, and C. Schlüchter (2006), Glacier response in the European Alps to Heinrich Event 1 cooling: The Gschnitz stadial, *J. Quat. Sci.*, *21*(2), 115–130.

Jansen, J. H. F., S. J. Van der Gaast, B. Koster, and A. J. Vaars (1998), CORTEX, a shipboard XRF-scanner for element analyses in split sediment cores, *Mar. Geol.*, *151*, 143–153.

Jones, G. A., and A. R. Gagnon (1994), Radiocarbon chronology of Black Sea sediments, *Deep Sea Res., Part I*, *41*(3), 531–557.

Jørgensen, B. B. (2003), Cruise 51, Leg 4, Istanbul-Istanbul, *METEOR-Ber.* 03–1, pp. 1–57, Max Planck Inst., Bremen, Germany.

Knutz, P. C., R. Zahn, and I. R. Hall (2007), Centennial-scale variability of the British Ice Sheet: Implications for climate forcing and Atlantic meridional overturning circulation during the last deglaciation, *Paleoceanography*, *22*, PA1207, doi:10.1029/2006PA001298.

Kroonenberg, S. B., G. V. Rusakov, and A. A. Svitoch (1997), The wandering of the Volga delta: A response to rapid Caspian sealevel change, *Sediment. Geol.*, *107*, 189–209.

Kvasov, D. (1979), The late-Quaternary history of large lakes and inland seas of Eastern Europe, *Ann. Acad. Sci. Fennicae*, *157*, 71 pp.

Kwiecien, O., H. W. Arz, F. Lamy, S. Wulf, U. Röhl, and G. H. Haug (2008), Reservoir ages of the glacial Black Sea, *Radiocarbon*, in press.

Lamy, F., H. W. Arz, G. C. Bond, A. Bahr, and J. Pätzold (2006), Multicentennial-scale hydrological changes in the Black Sea and northern Red Sea during the Holocene and the Arctic/North Atlantic Oscillation, *Paleoceanography*, *21*, PA1008, doi:10.1029/2005PA001184.

Major, C., W. Ryan, G. Lericolais, and I. Hajdas (2002), Constraints on Black Sea outflow to the Sea of Marmara during the last glacial-interglacial transition, *Mar. Geol.*, *190*, 19–34.

Major, C. O., S. L. Goldstein, W. B. F. Ryan, G. Lericolais, A. M. Piotrowski, and I. Hajdas (2006), The co-evolution of Black Sea level and composition through the last deglaciation and its paleoclimatic significance, *Quat. Sci. Rev.*, *25*(17–18), 2031–2047.

Majoran, S., S. Agrenius, and G. S. Dwyer (1999), The effect of temperature on the geochemical composition of the shells of the ostracod species Krithe praetexta praetexta, *GEOSOUND*, *35*, 93–113.

Mangerud, J., M. Jakobsson, H. Alexanderson, V. Astakhov, G. K. C. Clarke, M. Henriksen, C. Hjort, G. Krinner, J.-P. Lunkka, and P. Moller (2004), Ice-dammed lakes and rerouting of the drainage of northern Eurasia during the Last Glaciation, *Quat. Sci. Rev.*, *23*(11–13), 1313–1332.

Manheim, F. T. and K. M. Chan (1974), Interstitial waters of Black Sea sediments: New data and review, in *The Black Sea—Geology, Chemistry and Biology*, edited by E. T. Degens and D. Ross, pp. 155–180, Am. Assoc. of Pet. Geol., Tulsa, Okla.

Ménot, G., E. Bard, F. Rostek, J. W. H. Weijers, E. C. Hopmans, S. Schouten, and J. S. S. Damste (2006), Early reactivation of European rivers during the last deglaciation, *Science*, *313*(5793), 1623–1625.

Morse, J. W., and M. Bender (1990), Partition coefficients in calcite: Examination of factors influencing the validity of experimental results and their application to natural systems*Chem. Geol.*, *82*, 265–277.

Mudie, P. J., A. Rochon, A. E. Aksu, and H. Gillespie (2002a), Dinoflagellate cysts, freshwater algae and fungal spores as salinity indicators in Late Quaternary cores from Marmara and Black seas, *Mar. Geol.*, *190*, 203–231.

Mudie, P. J., A. Rochon, and A. E. Aksu (2002b), Pollen stratigraphy of Late Quaternary cores from Marmara Sea: Land-sea correlation and paleoclimatic history, *Mar. Geol.*, *190*, 233–260.

Mudie, P. J., A. Rochon, A. E. Aksu, and H. Gillespie (2003), Late glacial, Holocene and modern dinoflagellate cyst assemblages in the Aegean-Marmara-Black Sea corridor: Statistical analysis and re-interpretation of the early Holocene Noah's Flood hypothesis, *Rev. Paleobot. Palynol.*, *2563*, 1–25.

Müller, A. (1999), Mg/Ca- und Sr/Ca-Verhältnisse in biogenem Carbonat planktischer Foraminiferen und benthischer Ostracoden, Ph.D. thesis, Univ. Kiel, Kiel, Germany.

Myers, P. G., C. Wielki, S. B. Goldstein, and E. J. Rohling (2003), Hydraulic calculations of postglacial connections between the Mediterranean and the Black Sea, *Mar. Geol.*, *201*, 253–267.

Öszoy, E., and Ü. Ünlüata (1997), Oceanography of the Black Sea: A review of some recent results, *Earth Sci. Rev.*, *42*, 231–272.

Öszoy, E., D. Rank, and I. Salihoglu (2002), Pycnocline and deep mixing in the Black Sea: Stable isotope and transient tracer measurements, *Estuarine Coastal Shelf Sci.*, *54*(3), 621–629.

Palacios-Fest, M. R., and D. L. Dettman (2001), Temperature controls monthly variation in ostracod valve Mg/Ca: Cypridopsis vidua from a small lake in Sonora, Mexico, *Geochim. Cosmochim. Acta*, *65*(15), 2499–2507.

Palacios-Fest, M., A. L. Carreno, J. R. Ortega-Ramirez, and G. Alvarado-Valdéz (2002), A paleoenvironmental reconstruction of Laguna Babicore, Chihuahua, Mexico based on ostracod paleoecology and trace element shell chemistry, *J. Paleolimnol.*, *27*, 185–206.

Panin, N., and D. Jipa (2002), Danube River sediment input and its interaction with the northwestern Black Sea, *Estuarine Coastal Shelf Sci.*, *54*, 551–562.

Pilcher, H., and W. Friedrich (1976), Radiocarbon dates of Santorini volcanics, *Nature*, *262*, 373–374.

Rasmussen, S. O., et al. (2006), A new Greenland ice core chronology for the last glacial termination, *J. Geophys. Res.*, *111*, D06102, doi:10.1029/2005JD006079.

Reimer, P. J., et al. (2004), IntCal04 terrestrial radiocarbon age calibration, 0–26 Cal kyr BP, *Radiocarbon*, *46*(3), 1029–1058.

Richter, T. O., S. van der Gaast, B. Koster, A. Vaars, R. Gieles, H. C. de Stigter, H. de Haas, and T. C. E. van Weering (2006), The Avaatech XRF Core Scanner: Technical description and applications to NE Atlantic sediments, in *New Techniques in Sediment Core Analysis*, edited by G. Rothwell, *Geol. Soc. Spec. Publ.*, *267*, 39–50.

Rinterknecht, V. R., et al. (2006), The last deglaciation of the southeastern sector of the Scandinavian Ice Sheet, *Science*, *311*(5766), 1449–1452.

Röhl, U., and L. J. Abrams (2000), High-resolution, downhole, and nondestructive core measurements from site 999 and 1001 in the Caribbean Sea: Application to the late Paleocene thermal maximum, *Proc. Ocean Drill. Program Sci. Results*, *165*, 191–203.

Ryan, W. B. F., W. C. Pitman, III, C. Major, K. Shimkus, V. Moskalenko, G. A. Jones, P. Dimitrov, N. Görür, M. Sakinc, and H. Yüce (1997), An abrupt drowning of the Black Sea shelf, *Mar. Geol.*, *138*, 119–126.

Ryan, W. B. F., C. O. Major, G. Lericolais, and S. L. Goldstein (2003), Catastrophic flooding of the Black Sea, *Annu. Rev. Earth Planet. Sci.*, *31*, 525–554.

Siani, G., M. Paterne, E. Michel, R. Sulpizio, A. Sbrana, M. Arnold, and G. Haddad (2001), Mediterranean Sea surface radiocarbon reservoir age changes since the Last Glacial Maximum, *Science*, *294*(5548), 1917–1920.

Sperling, M., G. Schmiedel, C. Hemleben, K. C. Emeis, H. Erlenkeuser, and P. M. Grootes (2003), Black Sea impact on the formation of eastern Mediterranean sapropel S1? Evidence from the Marmara Sea, *Palaeogeogr. Palaeoclimatol. Palaeoecol.*, *190*, 9–21.

Stuiver, M., and A. Reimer (1993), Extended ^{14}C data base and revised CALIB 3.014C age calibration program, *Radiocarbon*, *35*, 215–230.

Svitoch, A. A. (1999), Caspian Sea level in the Pleistocene: Hierarchy and position in the paleogeographic and chronological records, *Oceanology*, *39*, 94–101.

Svitoch, A. A. (2007), On the nature of the Khvalynian Transgression of the Caspian Sea, *Oceanology*, *47*, 282–289.

Swart, P. K. (1991), Factors affecting the oxygen isotopic composition of the Black Sea, in *Black Sea Oceanography*, edited by E. Izdar and J. W. Murray, pp. 75–88, Kluwer, Dordrecht, Netherlands.

Vinther, B. M., et al. (2006), A synchronized dating of three Greenland ice cores throughout the Holocene, *J. Geophys. Res.*, *111*, D13102, doi:10.1029/2005JD006921.

von Grafenstein, U., H. Erlenkeuser, A. Brauer, J. Jouzel, and S. Johnsen (1999a), A mid-European decadal isotope-climate record from 15,500 to 5000 years B. P., *Science*, *284*, 1654–1657.

von Grafenstein, U., H. Erlenkeuser, and P. Trimborn (1999b), Oxygen and carbon isotopes in modern fresh-water ostracod valves: Assessing vital offsets and autecological affects of interest for palaeoclimate studies, *Palaeogeogr. Palaeoclimatol. Palaeoecol.*, *148*, 133–152.

von Grafenstein, U., U. Eicher, H. Erlenkeuser, P. Ruch, J. Schwander, and B. Ammann (2000), Isotope signature of the Younger Dryas and two minor oscillations at Gerzensee (Switzerland): Palaeoclimatic and palaeolimnologic interpretation based on bulk and biogenic carbonates, *Palaeogeogr. Palaeoclimatol. Palaeoecol.*, *159*, 215–229.

Wansard, G. (1996), Quantification of paleotemperature changes during isotopic stage 2 in the La Draga continental sequence (NE Spain) based on the Mg/Ca ratio of freshwater ostracods, *Quat. Sci. Rev.*, *15*(2–3), 237–245.

Wansard, G., and J. P. Roca (1997), Ètude expérimentale de l'incorporation du strontium et du magnesium dans le valves d'un ostracode d'eau douce, Heterocypris brevicaudata (Crustacea, Ostracoda), *C. R. Acad. Sci., Ser. II*, *325*, 403–409.

Wansard, G., P. De Deckker, and R. Julia (1998), Variability in ostracod partition coefficients D(Sr) and D(Mg): Implications for lacustrine palaeoenvironmental reconstructions, *Chem. Geol.*, *146*(1–2), 39–54.

Wansard, G., J. P. Roca, and F. Mezquita (1999), Experimental determination of strontium and magnesium partitioning in calcite of the freshwater ostracod Herpetocypris intermedia, *Arch. Hydrobiol.*, *145*, 237–253.